Contribution from the Laboratoire de Catalyse et de Chimie Fine,
Ecole Nationale Supérieure de Chimie, and GITER-CNRS, 31077 Toulouse Cêdex, France

Preparation and Characterization of the Dimetallo Ketone Complexes $Ir_2(\mu\text{-S-}t\text{-Bu})_2(\mu\text{-CO})L_2(CO)_2I_2$: Crystal and Molecular Structure of the Complex Where L = PMe_3

Carmen Claver,[†] Joëlle Fis,[†] Philippe Kalck,*[†] and Joël Jaud[‡]

Received July 29, 1986

Fast addition of 1 mol of iodine immediately after the addition of 2 mol of phosphorus ligands to $Ir_2(\mu\text{-S-}t\text{-Bu})_2(CO)_4$ induces, in the case of very basic ligands, the formation of the complexes $Ir_2(\mu\text{-S-}t\text{-Bu})_2(\mu\text{-CO})L_2(CO)_2I_2$. These complexes were characterized by IR and ^1H, ^{13}C, and ^{31}P NMR spectroscopy. An X-ray structural determination of the complex $Ir_2(\mu\text{-S-}t\text{-Bu})_2(\mu\text{-CO})(PMe_3)_2(CO)_2I_2$ was undertaken. Although the crystals decompose under the X-ray beam, the structure was refined to $R = 0.057$ and $R_w = 0.065$ on the basis of 2967 unique observed reflections and 153 parameters varied. This complex crystallizes in the monoclinic system space group $P2_1/c$ with $Z = 4$, $a = 16.445$ (6) Å, $b = 15.812$ (6) Å, $c = 15.244$ (7) Å, and $\beta = 110.6$ (2)°. The two iridium atoms are bridged by two thiolato ligands and a CO ligand for which the geometry is in agreement with a dimetallo ketone. The iridium–iridium distance is 3.115 (1) Å.

Introduction

There is a considerable current interest in using dinuclear complexes as templates for the activation of small molecules especially with intent to use those in homogeneous catalysis or to understand the mechanisms of the catalytic steps. In such a context the search for a cooperative effect between two metal centers appears as an interesting approach to gain more activity or quite unexpected reactivities when compared to a single metal center.[1]

Recent studies on thiolato-bridged homobimetallic species have shown that the $Rh_2(\mu\text{-S-}t\text{-Bu})_2(CO)_2L_2$ complexes and their iridium analogues present an unexpected reactivity toward small molecules.[2-7] The iridium series seems particularly attractive because model compounds can be obtained and be, a priori, mimetic of the intermediate species that can be responsible for the catalytic activity of the rhodium complexes. For the $Ir_2(\mu\text{-S-}t\text{-Bu})_2(CO)_2L_2$ complexes it was recently shown that the addition of 1 mol of iodine proceeds very quickly, presumably through a radical process, leading to an Ir(II)–Ir(II) complex.[4] Moreover a study on the mechanism of the phosphine addition to the starting material $Ir_2(\mu\text{-S-}t\text{-Bu})_2(CO)_4$ (**1**) has revealed two quite unexpected intermediate species that both present the $RS\text{–}Ir^{II}(\mu\text{-SR})(\mu\text{-CO})Ir^{II}$ core, resulting from a single cleavage of one of the two thiolato bridging ligands. In solution, when the terminal SR group again reaches the bridging position, the μ-CO ligand is evolved.

In this paper we report the reproducible preparation of the $Ir_2(\mu\text{-S-}t\text{-Bu})_2(\mu\text{-CO})(CO)_2L_2I_2$ complexes when fast addition of 1 mol of iodine is carried out just after the addition of PMe_3 or PMe_2Ph to the $Ir_2(\mu\text{-S-}t\text{-Bu})_2(CO)_4$ starting complex. Their characterization is also supported by an X-ray structure performed on the PMe_3 complex.

Experimental Section

All reactions were carried out under a dry and oxygen-free dinitrogen atmosphere with Schlenk tubes and vacuum-line procedures. Solvents were dried and freed of molecular oxygen. Microanalyses were performed by the "Service Central de Microanalyses du CNRS". Infrared spectra were recorded in toluene or dichloromethane solutions or in cesium bromide pellets on a Perkin-Elmer 1710 infrared Fourier transform spectrometer. ^1H NMR spectra were obtained at 90 MHz on a Bruker WH 90 FT spectrometer; chemical shifts were measured with respect to internal tetramethylsilane and are given in parts per million downfield positive. ^{31}P NMR were measured at 86.4 MHz on a Bruker WH 90FT spectrometer; chemical shifts were measured with respect to external H_3PO_4 and are given in parts per million downfield positive. ^{13}C NMR spectra were recorded at 62.86 MHz on a Bruker WM 250FT instrument using tetramethylsilane as internal standard. The starting material $Ir_2(\mu\text{-S-}t\text{-Bu})_2(CO)_4$ was prepared as previously reported.[8] Hexachloroiridic acid was obtained from Johnson-Matthey, and trimethylphosphine and dimethylphenylphosphine were purchased from Fluka AG.

Preparation of Compounds. (a) $Ir_2(\mu\text{-S-}t\text{-Bu})_2(\mu\text{-CO})(PMe_3)_2(CO)_2I_2$. Trimethylphosphine (91 μL, 0.888 mmol) and immediately afterward iodine (113 mg, 0.444 mmol) were added to a solution of $Ir_2(\mu\text{-S-}t\text{-Bu})_2(CO)_4$ (300 mg, 0.444 mmol)[8] in toluene (10 mL) at room temperature. After about 10 min of agitation, a yellow-orange precipitate appeared. After complete precipitation the product was filtered off, washed with hexane, and dried under reduced pressure. Crystals obtained in various solvents (e.g. CH_2Cl_2, toluene, THF, etc.) decomposed rapidly in the X-ray beam. X-ray stable yellow-orange crystals were obtained by crystallization in toluene and redissolving in acetone and were recrystallized by layering a slow diffusion of hexane at −25 °C. The IR spectra of these crystals show ν_{CO} bands in CsBr pellets at 2046 (vs), 2030 (s), and 1710 (s) cm^{-1}. Pale yellow microcrystalline materials were also found in small quantities in addition to the previous crystals; they present in CsBr three ν_{CO} bands at 2050 (vs), 2036 (vs), and 1718 (s) cm^{-1}. Typical yields were 80–85%. ^1H NMR ($CDCl_3$): δ 1.67 (s) (S-*t*-Bu endo), 1.88 (s) (S-*t*-Bu exo), 1.87 (d, $^2J_{PH} = 11.4$ Hz) (PMe_3). ^{31}P NMR ($CDCl_3$): δ − 55.9 (s) (PMe_3). ^{13}C NMR ($CDCl_3$): δ 31.8 (S–C–*C* endo), 32.1 (S–C–*C* exo), 46.1 (S–*C* endo), 57.0 (S–*C* exo), 16.7 (d, $J_{PC} = 42.6$ Hz, PMe_3), 128.7 (d, $^2J_{PC} = 17.6$ Hz, CO), 125.4 (μ-CO). Anal. Calcd: C, 19.39; H, 3.45; S, 6.09; I, 24.11. Found: C, 20.30; H, 3.44; S, 5.99; I, 23.52.

(b) $Ir_2(\mu\text{-S-}t\text{-Bu})_2(\mu\text{-CO})(PMe_2Ph)_2(CO)_2I_2$. Dimethylphenylphosphine (63.3 μL, 0.444 mmol) followed immediately by iodine (56.42 mg, 0.222 mmol) was added to $Ir_2(\mu\text{-S-}t\text{-Bu})_2(CO)_4$ (150 mg, 0.222 mmol) dissolved in 10 mL of toluene. The solution was stirred for 2 h, giving a small amount of red-orange precipitate. The product was filtered off, washed with hexane, and dried under vacuum. All attempts to obtain crystals were unsuccessful. Variable amounts of $Ir_2(\mu\text{-S-}t\text{-Bu})_2(PMe_2Ph)_2(CO)_2I_2$[4] were systematically observed as shown by the results of various elemental analyses. The IR spectrum shows three ν_{CO} bands at 2045 (vs), 2034 (s), and 1711 (s) cm^{-1} along with the two ν_{CO} bands at 2007 (vs) and 1990 (m) cm^{-1} characteristic of $Ir_2(\mu\text{-S-}t\text{-Bu})_2(CO)_2(PMe_2Ph)_2I_2$. Typical yields were 75–80%. ^1H NMR ($CDCl_3$): δ 1.56 (s) (S-*t*-Bu endo), 1.73 (s) (S-*t*-Bu exo), 2.16 (d), 1.99 (d, $^2J_{PH} = 10.2$ Hz, P*Me*$_2$Ph). ^{31}P NMR ($CDCl_3$): δ −40.8 (s) (PMe_2Ph). ^{13}C NMR ($CDCl_3$): δ 31.7 (S–C–*C*), 46.3 (S–*C* endo), 56.7 (S–*C* exo), 17.6 (PMe_2Ph), 14.6 (PMe_2Ph).

X-ray Data Collection. A yellow-orange crystal of $Ir_2(\mu\text{-S-}t\text{-Bu})_2(\mu\text{-CO})(PMe_3)_2(CO)_2I_2$ having approximate dimensions of 0.06 × 0.25 ×

[†] ENSC.
[‡] GITER-CNRS.

(1) See, for instance (a) Pignolet, L. H. *Homogeneous Catalysis with Metal Phosphine Complexes*; Plenum: New York 1983. (b) Krause, M. J.; Muetterties, E. L.; *Angew. Chem., Int. Ed. Engl.* **1983**, *22*, 135.
(2) Mayanza, A.; Bonnet, J. J.; Galy, J.; Kalck, P.; Poilblanc, R. *J. Chem. Res., Miniprint* **1980**, 2101.
(3) Bonnet, J. J.; Thorez, A.; Maisonnat, A.; Galy, J.; Poilblanc, R. *J. Am. Chem. Soc.* **1979**, *101*, 5940.
(4) Kalck, P.; Bonnet, J. J. *Organometallics* **1982**, *1*, 1211.
(5) Guilmet, E.; Maisonnat, A.; Poilblanc, R. *Organometallics* **1983**, *2*, 1123.
(6) El Amane, M.; Mathieu, R.; Poilblanc, R. *Organometallics* **1983**, *2*, 1618.
(7) El Amane, M.; Maisonnat, A.; Dahan, F.; Pince, R.; Poilblanc, R. *Organometallics* **1985**, *4*, 773.
(8) De Montauzon, D.; Poilblanc, R. *Inorg. Synth.* **1980**, *20*, 236.

0020-1669/87/1326-3479$01.50/0

Table I. Crystallographic Experimental Details

A. Crystal Data

formula: $C_{17}H_{36}Ir_2I_2O_3P_2S_2$	a = 16.445 (6) Å
fw: 1052.76	b = 15.812 (6) Å
F(000): 2128	c = 15.244 (7) Å
cryst dimens: 0.06 × 0.25 × 0.27 mm	β = 110.6 (2)°
Mo Kα radiation: λ = 0.71073 Å	V = 3709 (2) Å^3
temp: 20 ± 1 °C	Z = 4
monoclinic space group $P2_1/c$	ρ = 1.885 g/cm^3
	μ = 89.96 cm^{-1}
	transmissn factor between 0.5701 and 0.1536 (mean value 0.4301)

B. Intensity Measurements

instrument	Enraf-Nonius CAD4 diffractometer
monochromator	graphite cryst, incident beam
attenuator	Zr foil, factor 19.4
takeoff angle	3.2°
detector aperture	4.0 mm horiz
	4.0 mm vert
cryst–detector dist	20.7 cm
scan type	θ–2θ
scan width	(0.9 + 0.350 tan θ)°
max 2θ	20°
no. of indep reflcns	2967 (1901 > 2σ(I))
collcd octants	$+h,+k,\pm l$

C. Structure Solution and Refinement

solution	Patterson + direct methods
hydrogen atoms	included as fixed contribution to the structure factor
anomalous dispersion	all non-hydrogen atoms
no. of reflcns included	1901
no. of params refined	153
unweighted agreement factor	R = 0.057[a]
weighted agreement factor	R_w = 0.065[b]
high peak in final diff map	0.25 e/Å^{-3}

[a] $R = \sum||k|F_o| - |F_c||/\sum k|F_o|$. [b] $R_w = [\sum w(kF_o - |F_c|)^2/\sum wk^2F_o^2]^{1/2}$ with $w = 4\ F_o^2/\sigma^2(F_o^2)$.

Table II. Selected Bond Distances (Å)[a]

Ir1–I1	2.831 (3)	O2–C2	1.16 (4)
Ir1–S1	2.437 (9)	O3–C3	1.24 (3)
Ir1–S2	2.431 (9)	Ir2–C2	1.77 (3)
C10–C11	1.53 (6)	S1–C3	2.71 (3)
Ir1–P1	2.319 (9)	Ir2–C3	2.00 (3)
C10–C12	1.49 (6)	S2–C3	2.83 (3)
S1–C10	1.86 (3)	C10–C13	1.45 (6)
P1–C4	1.82 (4)	C14–C15	1.51 (5)
Ir1–C1	1.73 (4)	P1–C5	1.76 (4)
C14–C16	1.47 (6)	S2–C14	1.91 (4)
Ir1–C3	2.00 (3)	P1–C6	1.77 (4)
C14–C17	1.53 (6)	P2–C7	1.73 (5)
Ir2–I2	2.865 (3)	P2–C8	1.75 (7)
Ir2–S1	2.421 (10)	P2–C9	1.77 (7)
Ir2–S2	2.425 (11)	O1–C1	1.23 (4)
Ir2–P2	2.318 (12)	O51–C51	1.190 (0)
		C51–C52	1.593 (0)
		C51–C53	1.540 (0)

[a] Numbers in parentheses are estimated standard deviations in the least significant digits.

0.27 mm was mounted on a CAD4 Enraf Nonius PDP 11/23 computer-controlled single-crystal diffractometer. The unit cell was refined by optimizing the setting of 25 (Mo Kα) reflections. The results are shown in Table I as well as the conditions for intensity measurements. All calculations were performed on a Digital VAX 730 computer using SDP.[9] The reflections were corrected for Lorentz–polarization factors; a numerical absorption correction was applied. The crystal is bounded by the 011, 01$\bar{1}$, and 100 faces. Several attempts to measure the intensities by normal scan were unsuccessful due to crystal decomposition in the X-ray beam. This problem was solved by measuring the diffraction data by successive shells of Bragg angles. However a strong isotropic decrease of reflections (62%) led us to effect a linear correction of the decrease as a function of time.

Structure Solution and Refinement. The structure was solved by deconvolution of the Patterson function in order to localize the two iridium atoms. Direct methods (Multan) were used to recycle these two atoms and locate the other atoms. In order to obtain a better data to parameters ratio only the atoms of iridium, iodine, sulfur, and phosphorus were refined with anisotropic thermal parameters. All the other atoms were refined only with isotropic thermal parameters. The hydrogen atoms were introduced in the last calculation in their expected positions with a C–H distance of 0.97 Å. The calculated positions were checked by a

(9) Frentz, B. A. In *Computing in Crystallography*; Schenk, H., Oethof-Harelkamp, K., Vankonigsveld, M., Bassi, G. C., Eds.; Delft University Press: Delft, Holland, 1978; pp 64–71.

Table III. Selected Bond Angles (deg)[a]

I1–Ir1–S1	104.0 (2)	P2–Ir2–C2	90 (1)
I1–Ir1–S2	93.5 (2)	P2–Ir2–C3	96.0 (9)
I1–Ir1–P1	90.3 (3)	C1–Ir1–C3	98 (2)
I2–Ir2–S1	104.0 (2)	I2–Ir2–S2	93.3 (2)
I1–Ir1–C1	83 (1)	I2–Ir2–P2	91.9 (2)
I1–Ir1–C3	172.2 (8)	C2–Ir2–C3	97 (1)
S1–Ir1–S2	78.6 (3)	S1–Ir1–P1	90.9 (3)
I2–Ir2–C2	84.3 (9)	I2–Ir2–C3	172.1 (9)
S1–Ir1–C1	172 (1)	S1–Ir2–S2	79.0 (3)
S1–Ir1–C3	74.8 (8)	S1–Ir2–P2	91.0 (4)
S2–Ir1–P1	169.5 (4)	S1–Ir2–C2	171.7 (9)
S2–Ir1–C1	103 (1)	S1–Ir2–C3	75.0 (9)
S2–Ir1–C3	78.8 (8)	S2–Ir2–P2	169.6 (4)
P1–Ir1–C1	87 (1)	S2–Ir2–C2	100 (1)
P1–Ir1–C3	97.4 (9)	S2–Ir2–C3	78.8 (9)
I2–Ir2–P2	91.9 (2)	I2–Ir2–C2	84.3 (9)
Ir1–S1–Ir2	79.7 (3)	Ir1–S1–C3	45.2 (7)
Ir1–S1–C10	120.0 (9)	Ir2–S1–C3	45.5 (6)
Ir2–S1–C10	120.0 (9)	C3–S1–C10	154.0 (9)
Ir1–S2–Ir2	79.7 (3)	Ir1–S2–C3	43.8 (6)
Ir1–S2–C14	114.0 (9)	C3–S2–C14	104.0 (9)

[a] Numbers in parentheses are estimated standard deviations in the least significant digits.

Table IV. Selected Positional and Thermal Parameters for $Ir_2(\mu\text{-S-}t\text{-Bu})_2(\mu\text{-CO})(PMe_3)_2(CO)_2I_2$

atom	x	y	z	B,[a] Å^2
Ir1	0.15203 (9)	0.08171 (9)	0.20240 (8)	2.88 (3)
Ir2	0.23204 (9)	−0.0978 (1)	0.25412 (9)	3.17 (3)
I1	0.1720 (2)	0.2379 (2)	0.2985 (2)	5.39 (7)
I2	0.3552 (2)	−0.1728 (2)	0.4186 (2)	5.99 (8)
S1	0.3005 (6)	0.0331 (6)	0.2357 (5)	3.2 (2)
S2	0.1768 (6)	−0.0014 (7)	0.3436 (6)	4.0 (2)
P1	0.1529 (6)	0.1513 (7)	0.0688 (5)	3.5 (2)
P2	0.2914 (7)	−0.1678 (7)	0.1573 (6)	4.6 (3)
O1	−0.036 (2)	0.119 (2)	0.143 (2)	5.7 (7)*
O2	0.129 (2)	−0.251 (2)	0.249 (2)	6.3 (7)*
O3	0.084 (1)	−0.066 (2)	0.080 (2)	4.7 (6)*
C1	0.043 (2)	0.106 (3)	0.167 (2)	5.0 (9)*
C2	0.169 (2)	−0.189 (2)	0.254 (2)	2.9 (7)*
C3	0.141 (2)	−0.036 (2)	0.151 (2)	1.9 (6)*
C4	0.143 (2)	0.080 (2)	−0.028 (2)	4.0 (8)*
C5	0.245 (2)	0.215 (3)	0.082 (3)	5 (1)*
C6	0.067 (3)	0.225 (3)	0.023 (3)	6 (1)*
C7	0.248 (4)	−0.143 (4)	0.039 (4)	10 (2)*
C8	0.403 (4)	−0.153 (4)	0.181 (4)	12 (2)*
C9	0.289 (4)	−0.280 (4)	0.166 (4)	12 (2)*
C10	0.391 (2)	0.078 (2)	0.336 (2)	3.6 (8)*
C11	0.374 (2)	0.080 (3)	0.428 (2)	4.8 (9)*
C12	0.408 (2)	0.165 (3)	0.313 (3)	5 (1)*
C13	0.467 (3)	0.025 (3)	0.351 (3)	7 (1)*
C14	0.073 (2)	−0.036 (2)	0.363 (2)	4.8 (9)*
C15	0.006 (2)	−0.070 (3)	0.275 (3)	5 (1)*
C16	0.046 (3)	0.042 (3)	0.399 (3)	6 (1)*
C17	0.104 (3)	−0.104 (3)	0.439 (3)	8 (1)*
O51	0.371	0.424	0.348	6.0
C51	0.322	0.480	0.314	6.0
C52	0.291	0.475	0.203	6.0
C53	0.294	0.548	0.370	6.0

[a] Starred values denote isotropically refined atoms. Values for anisotropically refined atoms are given in the form of the isotropic equivalent thermal parameter defined as $^4/_3[a^2\beta(1,1) + b^2\beta(2,2) + c^2\beta(3,3) + ab(\cos\gamma)\beta(1,2) + ac(\cos\beta)\beta(1,3) + bc(\cos\alpha)\beta(2,3)]$.

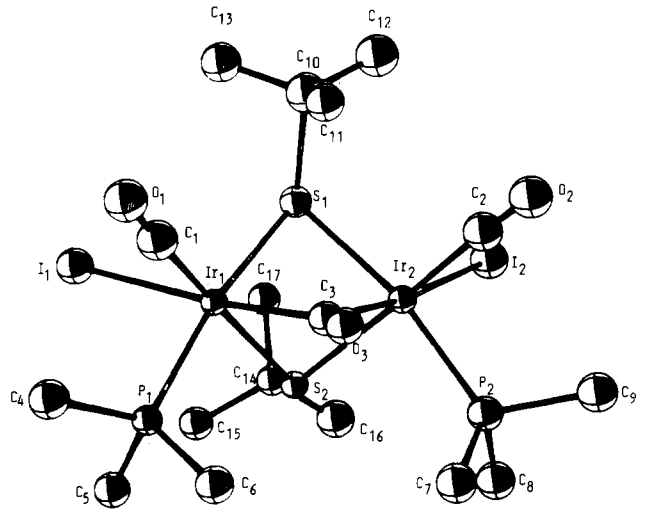

Figure 1. ORTEP drawing of $Ir_2(\mu\text{-S-}t\text{-Bu})_2(\mu\text{-CO})(PMe_3)_2(CO)_2I_2$ with 50% thermal ellipsoids.

difference Fourier map. This permitted location of one solvent molecule whose positional parameters were fixed. Scattering factors were taken from Cromer and Waber.[10] Anomalous dispersion effects were included in F_c,[11] and their values were those of Cromer and Liberman.[12] An ORTEP diagram of the molecular structure is shown in Figure 1. Final positional and thermal parameters are given in Table IV. Selected interatomic distances and angles are listed in Tables II and III.

Results and Discussion

Preparation of the Complexes. The addition of 2 mol of phosphine or phosphite ligands must be followed immediately by the addition of 1 mol of iodine, which is introduced in the solid form so that the reaction is controlled by its dissolution. Thus the formation of small quantities of $Ir_2(\mu\text{-S-}t\text{-Bu})_2(CO)_4I_2$[4] is avoided. All of the reactions were performed in toluene. With trimethyl- and dimethylphenylphosphine the dimetallo ketone complexes are obtained, $Ir_2(\mu\text{-S-}t\text{-Bu})_2(\mu\text{-CO})(CO)_2L_2I_2$ (L = PMe_3 (**2a**); L = PMe_2Ph (**2b**)). However for less basic ligands, the reaction exclusively leads to the known dicarbonyl complexes **3**;[4] the reaction is quite the same as the direct addition of iodine to $Ir_2(\mu\text{-S-}t\text{-Bu})_2(CO)_2L_2$ complexes **4**. Elemental analyses were in agreement with the proposed formula for **2a** whereas for the PMe_2Ph analogue **2b** a small amount of **3b** was systematically observed.

Infrared spectra of **2a** in the solid state show two ν_{CO} stretching frequencies at 2046 (vs) and 2030 (vs) cm^{-1} for the terminal CO's and a low ν_{CO} band at 1710 (s) cm^{-1} indicative of a bridging CO ligand. For the iridium(I) complex $Ir_2(\mu\text{-S-}t\text{-Bu})_2(CO)_2(PMe_3)_2$ (**4a**),[13] the infrared bands for the two CO ligands are 1941 (vs) and 1927 (vs) cm^{-1} in the solid state. The two CO stretching frequencies were found at 1995 (vs) and 1977 (m) cm^{-1} for the iridium(II) diiodo complex **3a**.[4] Compared to **4a** and to **3a**, complex **2a** shows a difference of about 100 and 50 cm^{-1}, respectively; thus, the iridium atoms should be in the +III oxidation state. That would mean that the bridging CO ligand has to be considered as a dimetallo ketone. In solution this structure is retained since the three ν_{CO} bands are observed at 2040 (vs), 2032 (vs), and 1710 (s) cm^{-1} in toluene.

All the NMR data (see Experimental Section) are in agreement with this first conclusion. Indeed, ^{31}P NMR spectra present a single signal at −55.9 ppm indicative of two equivalent phosphorus ligands attached to two iridium(III) metal centers since the shifts are found at −44 ppm for **3a** (iridium(II))[4] and −29 ppm for **4a** (iridium(I)).[10] Moreover two *tert*-butyl signals are found: ^1H, δ = 1.67 (s) and 1.88 (s); ^{13}C, δ = 31.8 (s) and 32.1 (s) (methyl carbon), 46.1 (s) (quaternary carbon in the endo position), and 57.0 (s) for the $SC(CH_3)_3$ in the exo position. For a discussion of the assignments of endo and exo C atoms, see ref 13. The trimethylphosphine ligand gives rise to an ^1H doublet at 1.87 ppm ($^2J_{PH}$ = 11.4 Hz) and a ^{13}C doublet at 16.74 ppm ($^2J_{PC}$ = 42.6 Hz). In ^{13}C NMR the two terminal CO's are detected at 128.7 ppm as a doublet ($^2J_{PC}$ = 17.6 Hz) and the bridging CO at 125.4 (s) ppm.

From all these data, we can assign a geometry involving a symmetry plane containing the two sulfur atoms and the bridging CO ligand. The two CO ligands are in mutual cis position. Similar data were obtained for complex **2b**, $Ir_2(\mu\text{-S-}t\text{-Bu})_2(\mu\text{-CO})(CO)_2(PMe_2Ph)_2I_2$, although, due to low solubility, the CO ligands were not detected in ^{13}C NMR.

In order to gain more information about the geometry of these two complexes, the X-ray crystal and molecular structure of **2a** was undertaken.

X-ray Structure. The crystal structure involves the packing of four discrete dinuclear molecules per unit cell. A perspective view of the molecule **2a** along with the labeling of the atoms is shown in Figure 1. Examination of the various results shows that, after all the corrections carried out, several atoms, especially the C7, C8, and C9 carbon atoms, present thermal coefficients very different from those generally observed in such compounds. However, no doubt can remain on the environment of the iridium atoms and the presence and the position of the bridging CO ligand, which were the aim of this investigation. Concerning the various distances and angles under interest we do not observe any anomaly. The molecule presents roughly a mirror plane as shown by the calculations on the medium plane S1–S2–C3–O3 and by the closely related distances that correspond to each other. Each iridium atom is in an octahedral environment, surrounded by the two sulfur and the carbon atoms of the bridging *t*-BuS and CO ligands and by three terminal ligands, namely iodine, carbon monoxide, and trimethylphosphine. One thiolato ligand and the PMe_3 ligand occupy roughly the two apical positions: the angle S1–Ir1–P1 is 169.5 (4)°. We could also consider the iodine atom and the C3 carbon atom being in the apical positions of the octahedron since, by loss of the bridging CO ligand, complex **3a** is obtained (vide infra) for which the iodine atom is the apical position of a square pyramid. This structure can conveniently be compared to those of $Ir_2(\mu\text{-S-}t\text{-Bu})_2(CO)_2(PMe_2Ph)_2I_2$ (**3b**) and $Ir_2(\mu\text{-S-}t\text{-Bu})_2(\mu\text{-CH}_2)(CO)_2(P(OMe)_3)_2I_2$.[7] All of the Ir–S, Ir–P, and Ir–I distances are slightly higher than those in **3b**, but quite comparable to those determined for the μ-CH_2 complex.[7] The iridium–iridium distance which was 2.702 (1) Å in **3b** is now 3.115 (1) Å in our complex; it is 3.1980 (4) Å in the μ-CH_2 complex.[7]

The important point seems to us the presence of the bridging CO ligand. Indeed the angles around the C3 atom are in agreement with a sp^2 environment for this carbon atom. We have to consider that the bridged CO ligand belongs to a dimetallo ketone complex and that no metal–metal bond is present. Usually a symmetrical carbonyl bridge presents a metal–carbon–metal angle of around 90° and requires the presence of a metal–metal bond.[14] Several metallo ketone complexes have already been characterized.[15–18] Interestingly in the A-frame complex $Rh_2(dpm)_2Cl_2(\mu\text{-CO})(\mu\text{-DMA})$ for which the CO ligand shows the same structure, the ^{13}C chemical shift has been found at 181 ppm;[15] it is 125 ppm here, whereas it is expected in the 200–240 ppm region for a classical bridging CO ligand.[19] Very recently

(10) Cromer, D. T.; Waber, J. T. *International Tables for X-ray Crystallography*; Kynoch: Birmingham, England, 1974; Vol. IV, Table 2.2.B.
(11) Ibers, J. A.; Hamilton, W. C. *Acta Crystallogr.* **1964**, *17*, 781.
(12) Cromer, D. T.; Liberman, D. *International Tables for X-ray Crystallography*; Kynoch: Birmingham, England, 1974; Vol. IV, Table 2.3.1.
(13) De Montauzon, D.; Kalck, P.; Poilblanc, R. *J. Organomet. Chem.* **1980**, *186*, 121.
(14) Cotton, F. A.; Wilkinson, G. *Advanced Inorganic Chemistry*, 4th ed.; Wiley: New York, 1980; pp 1052–1055.
(15) Cowie, M.; Southern, T. G. *J. Organomet. Chem.* **1980**, *193*, C46. Cowie, M.; Dwight, S. K. *Inorg. Chem.* **1980**, *19*, 2500.
(16) Cotton, R.; Mc Cormick, M. J.; Pannan, C. D. *Aust. J. Chem.* **1977**, *32*, 1425; *J. Chem. Soc., Chem. Commun.* **1977**, 823.
(17) Brown, M. P.; Puddephatt, R. J.; Rashidi, M.; Seddon, K. R. *J. Chem. Soc., Dalton Trans* **1978**, 1540. Brown, M. P.; Keith, A. N.; Manojlovic-Muir, L.; Muir, K. W.; Puddephatt, R. J.; Seddon, K. R. *Inorg. Chim. Acta* **1979**, *34*, L223.
(18) Kubiak, C. P.; Woodcock, C.; Eisenberg, R. *Inorg. Chem.* **1982**, *21*, 2119; *J. Am. Chem. Soc.* **1980**, *102*, 8637.

a value of 116 ppm was found for (OEP)Rh(μ-CO)RhOEP (OEP = octaethylporphyrin ligand).[20] Thus, such a dimetallo ketone bridging CO ligand requires σ bonds between the metals and the carbon atom so that the oxidation state of iridium is formally +III.

Stability of Complex 2a. The two complexes **2a** and **2b** are thermally resistant. Indeed after a week in boiling benzene only half of the complexes were converted into the complexes **3a** and **3b** by loss of a CO ligand. The reverse addition of CO to **3a** was not observed under the ambient conditions since no traces of **2a** were detected by infrared. Moreover, addition of Me_3NO to assist the decarbonylation of complex **2a** increased the CO loss only slightly even in boiling benzene. However we noted that exposure of complex **2a** to natural light in solution or even in the solid state gives rise to a very fast extrusion of the bridging CO ligand to form complex **3a**. Irradiation of solutions with sunlight is a good way to obtain **3a** from **2a** in a few minutes.

Mechanism of the Formation of 2a and 2b. Clearly, the formation of the μ-CO ligand in the complexes under interest is due to the fast attack of iodine to an intermediate species formed after the addition of phosphine. Indeed the addition of iodine to Ir_2(μ-S-*t*-Bu)$_2$(CO)$_4$ to give Ir_2(μ-S-*t*-Bu)$_2$(CO)$_4$I$_2$ and to Ir_2(μ-S-*t*-Bu)$_2$(CO)$_2$L$_2$ giving Ir_2(μ-S-*t*-Bu)$_2$(CO)$_2$L$_2$I$_2$ was shown to proceed very quickly. In this study, these two complexes were not detected by infrared even at the beginning of the reaction. Complex (CO)$_2$(PMe$_3$)(S-*t*-Bu)Ir(μ-S-*t*-Bu)Ir(CO)$_2$(PMe$_3$) (**5**) was previously proposed as an intermediate to explain the formation of two intermediate species characterized by X-ray, Ir_2(μ-S-*t*-Bu)(μ-CO)(CO)$_2$(PMe$_3$)$_2$(S-*t*-Bu) and Ir_3(μ-S-*t*-Bu)$_3$(μ-CO)(CO)$_4$(PMe$_3$)$_2$, when 2 equiv of trimethylphosphine are added to **1**.[21] The attack of iodine on complex **5** is believed to proceed very fast and through a radical process, as initially shown by Osborn on mononuclear complexes[22] and proposed for the formation of complexes **3**.[13] Presumably a first attack of iodine on a single iridium atom of **5** occurs to give I$^\bullet$ and [(CO)$_2$(PMe$_3$)(S-*t*-Bu)Ir(μ-S-*t*-Bu)Ir(CO)$_2$(PMe$_3$)I]$^\bullet$ (**6**), a d^8-d^7 species. Very recently Stobart et al. have shown that a d^8-d^7 complex could be isolated resulting from the oxidative addition of iodine to the complex Ir_2(μ-pyrazolato)$_2$(1,5-C$_8$H$_{12}$)$_2$.[23] We suggest that in this species **6** an internal attack of a carbonyl ligand coordinated to the d^7 iridium atom on the Ir(I) atom, with simultaneous loss of a terminal CO ligand, gives rise to the d^7-d^6 species **7**, [(CO)(PMe$_3$)(S-*t*-Bu)Ir(μ-S-*t*-Bu)(μ-CO)Ir(CO)(PMe$_3$)I]$^\bullet$. Finally a second radical process of **7** with I$^\bullet$ or with I_2 generates complex **2**.

Acknowledgment. ATOCHEM Co. is gratefully acknowledged for financial support and for a grant to J.F. We also thank the CNRS through the operation "GRECO Oxydes de Carbone" and the "Ministerio de Education y Ciencia" of Spain for a grant to C.C. We are indebted to Dr. J. Galy (Giter-CNRS) for helpful discussions.

Registry No. **1**, 63312-27-6; **2a**, 109839-53-4; **2b**, 109839-52-3.

Supplementary Material Available: Listings of anisotropic general temperature factors, root-mean-square amplitudes of thermal vibrations, least-squares planes, bond angles, and hydrogen atom positional and isotropic thermal parameters (9 pages); a listing of calculated and observed structure factors (22 pages). Ordering information is given on any current masthead page.

(19) Mann, B. E.; Taylor, B. B. *^{13}C NMR Data for Organometallic Compounds*; Academic: New York, 1981; Table 2.8.
(20) Wayland, B. B.; Woods, B. A. ;Coffin U. L. *Organometallics* **1986**, *5*, 1059.
(21) Kalck, P.; Bonnet, J. J. ; Poilblanc, R. *J. Am. Chem. Soc.* **1982**, *104*, 3069.
(22) Bradley, J. S.; Connor, D. E.; Osborn, J. A. *J. Am. Chem. Soc.* **1972**, *94*, 4043.
(23) Fjeldsted, D. O. X.; Stobart, S. P.; Zaworotko, M. G. *J. Am. Chem. Soc.* **1985**, *107*, 8258. Harrison, D. G.; Stobart, S. R. *J. Chem. Soc., Chem. Commun.* **1986**, 285.

Contribution from the Departamento de Quimica Inorganica, Instituto de Ciencia de Materiales de Aragon, Universidad de Zaragoza—CSIC, 50009 Zaragoza, Spain, and Department of Chemistry and Laboratory for Molecular Structure and Bonding, Texas A&M University, College Station, Texas 77843

Heterotrinuclear Pt_2Ag Clusters with Pt-Ag Bonds Unsupported by Covalent Bridges. Molecular Structures of $(NBu_4)_2[Pt_2(\mu\text{-}Cl)_2(C_6F_5)_4]$ and $(NBu_4)[Pt_2AgCl_2(C_6F_5)_4O(C_2H_5)_2]$

Rafael Uson,*† Juan Fornies,† Milagros Tomas,† Jose M. Casas,† F. Albert Cotton,*‡ and L. R. Falvello‡

Received May 13, 1987

The preparation and properties of new trinuclear (Pt_2Ag) clusters are reported. The compounds $(NBu_4)[Pt_2AgX_2(C_6F_5)_4OEt_2]$ (X = Cl (**1**), Br (**2**)) are formed by reaction of $(NBu_4)_2[Pt_2(\mu\text{-}X)_2(C_6F_5)_4]$ with $AgClO_4$ in dichloromethane/diethyl ether solution. The phosphine-substituted products $(NBu_4)[Pt_2Ag(\mu\text{-}Cl)_2(C_6F_5)_4L]$ (L = PPh_3 (**3**), $PMePh_2$ (**4**)) are formed by the reaction of $(NBu_4)_2[Pt_2(\mu\text{-}Cl)_2(C_6F_5)_4]$ with $AgOClO_3L$ at −30 °C. Product **3** is also formed by the reaction of **1** with PPh_3 in dichloromethane at −30 °C. The products were characterized by elemental analysis, conductance measurements, and IR spectroscopy. The precursor $(NBu_4)_2[Pt_2(\mu\text{-}Cl)_2(C_6F_5)_4]$ and product **1**, $(NBu_4)[Pt_2Ag(\mu\text{-}Cl)_2(C_6F_5)_4OEt_2]$, were analyzed by X-ray diffraction. Crystals of $(NBu_4)_2[Pt_2(\mu\text{-}Cl)_2(C_6F_5)_4]$ are monoclinic, space group $P2_1/c$, with a = 12.763 (4) Å, b = 12.858 (4) Å, c = 19.554 (7) Å, β = 104.62 (2)°, V = 3105 (2) Å^3, and Z = 2. The structure was refined to residuals of R = 0.0399, R_w = 0.0525, and quality-of-fit = 1.044, with 370 parameters and 2960 data. The $Pt_2Cl_2C_4$ core of the complex anion is planar. Crystals of product **1** are monoclinic, space group $P2_1/n$, with a = 12.574 (2) Å, b = 14.749 (2) Å, c = 27.983 (3) Å, β = 92.73 (1)°, V = 5184 (2) Å^3, and Z = 4. The structure was refined to final residuals of R = 0.0397, R_w = 0.0448, and quality-of-fit = 1.088, with 640 parameters and 4252 observations. While there is no direct Pt-Pt bond in **1**, the two Pt-Ag bonds are unbridged and have bond lengths of 2.782 (1) and 2.759 (1) Å. There are no close contacts between the silver atom and the fluorine atoms of the C_6F_5 ligands.

Introduction

For several years we have been studying the reactions between anionic (perhalophenyl)platinum(II) complexes, which behave as nucleophiles because of their negative charges, and suitable silver salts ($AgClO_4$, $AgNO_3$, or $R_3PAgOClO_3$), which serve as the electrophilic complements, although they can also act as halide abstractors. To date, we have observed and reported the following results.

1. An anionic Pt complex that contains no halide ligand ($[Pt(C_6F_5)_3(SC_4H_8)]^-$) reacts with a silver salt (eq 1) to give a

$$(NBu_4)[Pt(C_6F_5)_3(SC_4H_8)] + O_3ClOAgP(C_6H_5)_3 \xrightarrow{CH_2Cl_2} NBu_4ClO_4 + [(SC_4H_8)(C_6F_5)_3PtAgP(C_6H_5)_3] \quad (1)$$

neutral binuclear complex with an unbridged Pt-Ag bond of length

†Universidad de Zaragoza—CSIC.
‡Texas A&M University.

0020-1669/87/1326-3482$01.50/0